Magnetoelastic coupling across the metamagnetic transition in $Ca_{2-x}Sr_xRuO_4$ ($0.2 \leq x \leq 0.5$)

J. Baier,[1] P. Steffens,[1] O. Schumann,[1] M. Kriener,[1,2] S. Stark,[1] H. Hartmann,[1] O. Friedt,[1] A. Revcolevschi,[3] P.G. Radaelli,[4] S. Nakatsuji,[2] Y. Maeno,[2] J.A. Mydosh,[1] T. Lorenz,[1] and M. Braden[1]

[1] *II. Physikalisches Institut, University of Cologne, Zülpicher Str. 77, 50937 Köln, Germany*
e-mail : braden@ph2.uni-koeln.de
[2] *Department of Physics, Kyoto University, Kyoto 606-8502, Japan*
[3] *Lab. de Physico-Chimie de l'État Solide, Université Paris-Sud, 91405 Orsay Cedex, France*
[4] *ISIS Facility, Rutherford Appleton Laboratory-CCLRC, Chilton, Didcot, Oxfordshire OX11 0QX, United Kingdom*

The magnetoelastic coupling in $Ca_{1.8}Sr_{0.2}RuO_4$ and in $Ca_{1.5}Sr_{0.5}RuO_4$ has been studied combining high-resolution dilatometer and diffraction techniques. Both compounds exhibit strong anomalies in the thermal-expansion coefficient at zero and at high magnetic field as well as an exceptionally large magnetostriction. All these structural effects, which are strongest in $Ca_{1.8}Sr_{0.2}RuO_4$, point to a redistribution of electrons between the different t_{2g} orbitals tuned by temperature and magnetic field. The temperature and the field dependence of the thermal-expansion anomalies in $Ca_{1.8}Sr_{0.2}RuO_4$ yield evidence for a critical end-point lying close to the low-temperature metamagnetic transition; however, the expected scaling relations are not well fulfilled.

PACS numbers: 78.70.Nx, 75.40.Gb, 74.70.-b

1. INTRODUCTION

The phase diagram of $Ca_{2-x}Sr_xRuO_4$ exhibits a rich variety of physical phenomena spanning the unconventional superconductor Sr_2RuO_4 to the antiferromagnetic Mott-insulator Ca_2RuO_4.[1,2,3,4] The essentially different

character of these physical ground states is quite outstanding in view of the fact that only the ionic radius on the Ca/Sr-site varies throughout this series. The $Ca_{2-x}Sr_xRuO_4$-phase diagram offers therefore the interesting possibility to tune through a Mott-transition by structural changes only. The smaller ionic radius of divalent Ca compared to that of divalent Sr induces a series of structural phase transitions characterized by rotations or tilts of the RuO_6-octahedra as it is typically observed in perovskites and related compounds. Such structural deformations have a strong impact on the electronic band structure since they modify the metal-oxygen hopping parameters and thereby the electronic band widths.[5,6] In $Ca_{2-x}Sr_xRuO_4$ the decrease of the Sr content x first stabilizes a rotation of the octahedra around the c axis and then, for $x \leq 0.5$, a tilting of the octahedra around an in-plane axis.[7] Further decrease of the Sr-content finally leads to the Mott-transition associated with another structural transition, across which the RuO_6 octahedra become flattened and their tilting increases.[7,8,9]

Remarkable physical properties were reported for the Sr-concentration range $0.2 \leq x \leq 0.5$, i.e. in the metallic phase close to the Mott transition.[8,9] Approaching the Sr content x=0.5 from higher values Nakatsuji et al. report a continuous increase of the low-temperature magnetic susceptibility reaching at x=0.5 a value 200 times larger than that of pure Sr_2RuO_4.[8,9] Furthermore, the electronic coefficient of the specific heat is exceptionally high, of the order of $C_p/T \sim 250\,\frac{\mathrm{mJ}}{\mathrm{mole\,K^2}}$,[8,9,10] well in the range of typical heavy fermion compounds. Inelastic neutron scattering has revealed strongly enhanced magnetic fluctuations[11] with a propagation vector of $\mathbf{q}\sim(0.2,0,0)$. The fluctuations in $Ca_{2-x}Sr_xRuO_4$ with x close to 0.5 are quite different from those in pure Sr_2RuO_4:[12,13] Although the magnetic instability observed for $x = 0.5$ is still incommensurate, its character is closer to ferromagnetism. The magnetic properties of the $Ca_{2-x}Sr_xRuO_4$-compounds with a Sr content close to 0.5 show some resemblance to localized electron systems; it has even been proposed that in these materials an orbital-selective Mott-transition occurs leaving a part of the 4d-electrons itinerant.[14] This proposal has initiated a strong debate concerning its theoretical basis as well as concerning its applicability to the phase diagram of $Ca_{2-x}Sr_xRuO_4$. It appears safe to assume however, that the γ-band associated with the d_{xy}-orbital exhibits a much smaller band width than that of the α- or β-band, since the rotation mainly influences the hybridization of the d_{xy}-electrons.[5,6]

Upon further decrease of the Sr-content the tilt transition occurs with an apparently strong impact on the magnetic properties. The low-temperature magnetic susceptibility rapidly decreases with increasing tilt and the electronic specific-heat coefficient is reduced but remains at a rather high level. Applying a magnetic field to $Ca_{1.8}Sr_{0.2}RuO_4$ at low temperature induces a

metamagnetic transition with a step-like increase of the magnetisation of about 0.4 μ_B per Ru. The metamagnetic transition field, H_{mm} sensitively depends on the direction of applied field; the transition occurs at 5.5 T when the field is applied along the c-direction[9] whereas values of 2 and 7 T are found for field directions along the a, b-plane.[15] The strong anisotropy of the metamagnetic transition field, in particular the difference for the two orthorhombic in-plane directions, suggests the relevance of spin orbit coupling. The metamagnetic transition in $Ca_{1.8}Sr_{0.2}RuO_4$ strongly resembles that observed in the double-layer ruthenate $Sr_3Ru_2O_7$, which has attracted special interest due to quantum-critical phenomena related with the end-point of the first-order metamagnetic transition.[16,17,18] Apart from the different basic structure, these two- and single-layer ruthenates possess similar structural characteristics, in particular, they both exhibit the structural deformation characterized by octahedra rotation around the c-axis.

In recent work, we have analyzed the structural aspects of the metamagnetism in $Ca_{2-x}Sr_xRuO_4$ by a combination of diffraction, of high-resolution thermal expansion, and of magnetostriction experiments.[19,20] These studies gave evidence of a change of the orbital arrangement driven by either temperature or magnetic field. The thermal-expansion anomalies observed at zero magnetic field illustrate an increase of the d_{xy} orbital occupation upon cooling, whereas the anomalies at high field point to a decrease of the d_{xy}-occupation upon cooling. Accordingly, the structural effects seen as a function of magnetic field at low temperature (diffraction and magnetostriction results) show that upon increasing magnetic field electrons are transferred from the d_{xz}- and d_{yz}-orbitals into the d_{xy}-orbital. In this work we have completed these studies for $Ca_{2-x}Sr_xRuO_4$ with $x = 0.2$ and $x = 0.5$ by additional diffraction studies and by high-resolution dilatometer measurements along different direction in longitudinal and transverse magnetic fields. In addition we have focused on the metamagnetic transition itself by collecting more data close to the critical field and by extending the measurements towards lower temperatures for $Ca_{1.8}Sr_{0.2}RuO_4$ where the metamagnetic transition is best defined.

2. EXPERIMENT

Single crystals of $Ca_{2-x}Sr_xRuO_4$ were grown by a floating-zone technique in image furnaces at Kyoto University ($x = 0.2$) and at Université Paris Sud ($x = 0.5$). Details of the preparation process are reported in reference [21] . In addition, powder samples of $Ca_{1.8}Sr_{0.2}RuO_4$ and $Ca_{1.5}Sr_{0.5}RuO_4$ were prepared following the standard solid-state reaction. The samples were from the same batches as those studied in Refs.[8,9] or characterized by x-ray

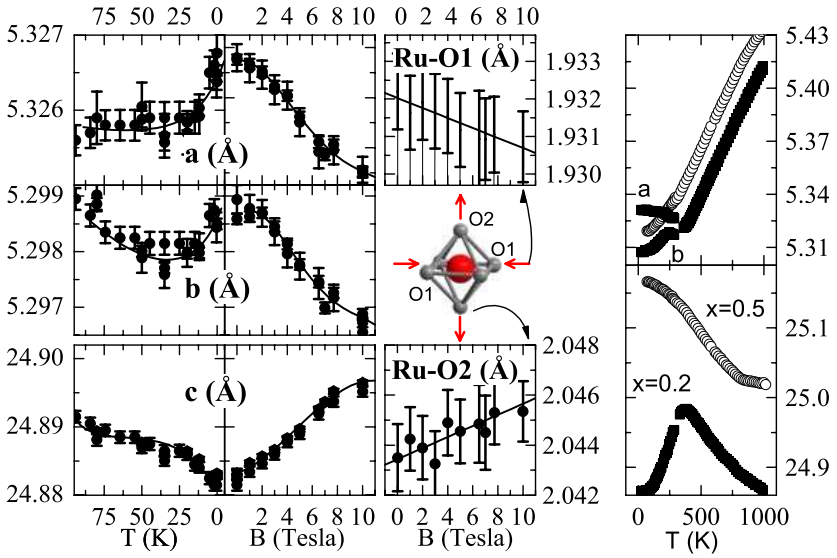

Fig. 1. Results of x-ray and neutron diffraction studies on $Ca_{1.8}Sr_{0.2}RuO_4$ and $Ca_{1.5}Sr_{0.5}RuO_4$. The left column gives the three orthorhombic lattice constants in $Ca_{1.8}Sr_{0.2}RuO_4$ as a function of temperature (results obtained on GEM); the middle columns show the lattice constants and the RuO bond lengths in $Ca_{1.8}Sr_{0.2}RuO_4$ as a function of magnetic field. The right column shows the a and b parameters (above) and the c lattice constant (below) for a wider temperature range for x=0.2 and 0.5. Note that $Ca_{1.8}Sr_{0.2}RuO_4$ exhibits a tetragonal to orthorhombic transition above room temperature whereas $Ca_{1.5}Sr_{0.5}RuO_4$ stays tetragonal down to about 50 K.

diffraction and susceptibility to possess identical properties.

Thermal expansion and magnetostriction were studied in magnetic fields up to 14 T in two different home-built capacitive dilatometers down to a lowest temperature of 300 mK.[22,23,24,25] The magnetization measurements were performed using a Quantum Design vibrating sample magnetometer (VSM). With the GEM diffractometer at the ISIS facility, neutron powder diffraction patterns were recorded as a function of temperature and in fields up to 10 T for $Ca_{1.8}Sr_{0.2}RuO_4$. X-ray powder diffraction patterns were recorded between 10 and 1000K using a D5000 Siemens diffractometer and Cu-K_α-radiation.

3. RESULTS AND DISCUSSION

3.1. Metamagnetic transition in $Ca_{1.8}Sr_{0.2}RuO_4$

Among the $Ca_{2-x}Sr_xRuO_4$ series the metamagnetic transition is best defined in $Ca_{1.8}Sr_{0.2}RuO_4$, therefore, we have chosen this composition for the most detailed thermodynamic studies. Figure 1 presents the results of diffraction experiments on a powder sample to characterize the structural evolution as function of temperature and magnetic field. These data were taken with the GEM diffractometer using a magnetic-field cryostat. In addition, the right panels of Figure 1 show the lattice parameters determined by x-ray diffraction in a wider temperature interval. $Ca_{1.8}Sr_{0.2}RuO_4$exhibits two distinct structural distortions at low temperatures, the rotation of the RuO_6-octahedrons around the c-axis and the tilting. Above ∼350 K, we find only the rotational distortion in space group $I4_1/acd$ with a lattice of $\sqrt{2} \cdot a, \sqrt{2} \cdot a, 2 \cdot c$ with respect to the ideal tetragonal lattice. A characteristic feature of this phase observed in many $Ca_{2-x}Sr_xRuO_4$-compounds[26] concerns the negative thermal expansion along the c-axis which persists over a broad temperature range, see the x-ray data in Fig. 1. The structural phase transition associated with the octahedra tilting further reduces the symmetry towards *Pbca* with the nearly same lattice parameters as in $I4_1/acd$. Although the *Pbca* space group has also been reported for the insulating and metallic phases observed for $x < 0.2$, see reference,[7] the symmetries are different, since in the case of the low-temperature phase for $x \geq 0.2$ the rotational distortion still leads to a doubling of the *c*-axis. High-resolution measurements of the thermal expansion along and perpendicular to the *c*-axis reveal strong low-temperature anomalies,[19] which are also visible in the diffraction data. Both in-plane parameters expand upon cooling whereas the c-axis shrinks, see figure 1. The diffraction data further show that upon increase of the magnetic field both in-plane directions shorten while *c* elongates. With the full structure analysis one may attribute this effect essentially to a change in the octahedron shape, which becomes elongated at high field indicating a shift of orbital occupation from d_{xy} to d_{xz} and d_{yz} states.[19]

A set of powder-diffraction patterns were recorded on GEM using a zero-field cryostat in order to better characterize the temperature dependence of the crystal structure in a wider range. Up to a temperature of 160 K the essential structural change arises from a weak variation of the tilt distortion. At low temperature the tilt angle saturates at values of 5.9 and 4.4 degrees determined at the basal (O1) and apical oxygen (O2), respectively. The minor differences in these two tilt angles indicate that the RuO_6-octahedrons are not perfect in $Ca_{1.8}Sr_{0.2}RuO_4$. The tilt distortion is coupled to the orthorhombic strain $a > b$ which at first sight is counterintuitive, as the

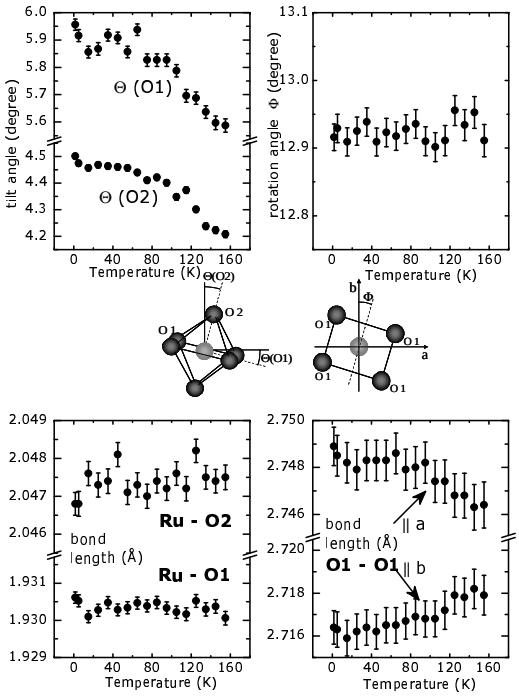

Fig. 2. Structural evolution of $Ca_{1.8}Sr_{0.2}RuO_4$ as determined by powder neutron diffraction on GEM without magnetic field, the structural results correspond to Rietveld-fits in space-group *Pbca*, but constraints had to be used to limit the number of free parameters.

tilt occurs around the *b*-axis which is the shorter one. Similar to other K_2NiF_4 materials with a tilt distortion, the interactions in the Ca/Sr-O rock-salt layer induce an elongation of the lattice and of the RuO_6-octahedron perpendicular to the tilt axis. Although this octahedral distortion might be relevant in splitting the d_{xz} and d_{yz}-t_{2g}-levels and hence cause the in-plane anisotropy of the metamagnetic transition field, it is not related to an orbital ordering effect. The orthorhombic splitting, as well as the difference in the O1-O1-edge lengths of the octahedrons, are clearly coupled to the tilt angles, see Fig. 1 and 2. The low-temperature anomalies seen in the thermal expansion[19] are clearly visible in the lattice parameters, but the effect in the internal crystal structure is within the error of this measurement, see Fig. 2.

Figure 3 shows the magnetostriction data recorded along the c-axis for field directions parallel and perpendicular to *c*. Qualitatively, both orientations show the same effect, – the elongation of the lattice when passing the metamagnetic transition at $H_{meta-magn}$=5.7 T for the field applied along *c* and at 2.0 T for the field perpendicular to *c*, see also reference.[19] At fields well above the metamagnetic transition, there is little quantitative difference

between the two field directions: the elongation is only 20% smaller when the field is applied parallel to c. The comparable structural effects along both directions imply that the magnetostriction of $Ca_{1.8}Sr_{0.2}RuO_4$ does not simply arise from the alignment of anisotropic ionic coordinations as it is the case in rare-earth compounds. Instead it has to be attributed to a transition or at least to a cross-over between distinct phases. Spin-orbit coupling seems to cause the sizeable anisotropy of the metamagnetic transition field, but it seems not to play a major role in the metamagnetic transition itself. The magnetostriction data and their field derivative show that the transition becomes smeared out with increasing temperatures. The maxima of the derivatives shift towards higher fields with increasing temperatures. Furthermore, the height of the peak in the magnetostriction rapidly decreases with increasing temperature for both field directions; roughly $\frac{1}{\lambda_{max}}$ scales with $(T^2 + const.)$, see Figure 2e) and f).

At the lowest temperature of 0.3 K, the magnetostriction along both field directions was measured upon increasing and decreasing field. There is no hysteresis discernible, which is surprising in view of the expected first-order character of the metamagnetic transition. Furthermore, even at the lowest temperature studied, the transition appears quite broad, in particular when compared to the metamagnetic transition in $Sr_3Ru_2O_7$, which consists of three contributions each of them possessing a width of the order of a tenth of a Tesla.[18,27] We cannot exclude that similar features are hidden in the broader peak in $Ca_{1.8}Sr_{0.2}RuO_4$ but one may note that the symmetry in $Ca_{1.8}Sr_{0.2}RuO_4$ is orthorhombic already at zero field. In $Ca_{2-x}Sr_xRuO_4$ the mixed occupation of Ca and Sr with distinct ionic radii induces strong intrinsic disorder with local variations of the tilt and rotation angles together with the concomitant local variation of the electronic structure. Evidence for local disorder in the $Ca_{2-x}Sr_xRuO_4$-series has recently been found in ARPES and STM studies.[28] The intrinsic disorder most likely is responsible for the broadening of the transition and it may further suppress any hysteresis. Keeping the strong microscopic disorder in mind it appears very difficult to determine the thermodynamic critical end-point in $Ca_{1.8}Sr_{0.2}RuO_4$ or even to discuss its existence at finite temperatures.

Figure 4 shows the results of the thermal-expansion measurements taken along the c-direction with the field parallel to c (longitudinal configuration). Both the thermal expansion coefficient $\alpha_c(T) = \frac{\partial c}{c \partial \mathrm{T}}$ and the length change $\Delta c/c$ are shown in the upper panels. One immediately recognizes that the strong thermal expansion anomaly occurring around 20 K changes its sign upon increase of the magnetic field in accordance with the idea that all these effects are due to the orbital rearrangement.[19] Here, we want to discuss whether the effects across the metamagnetic transition in $Ca_{1.8}Sr_{0.2}RuO_4$

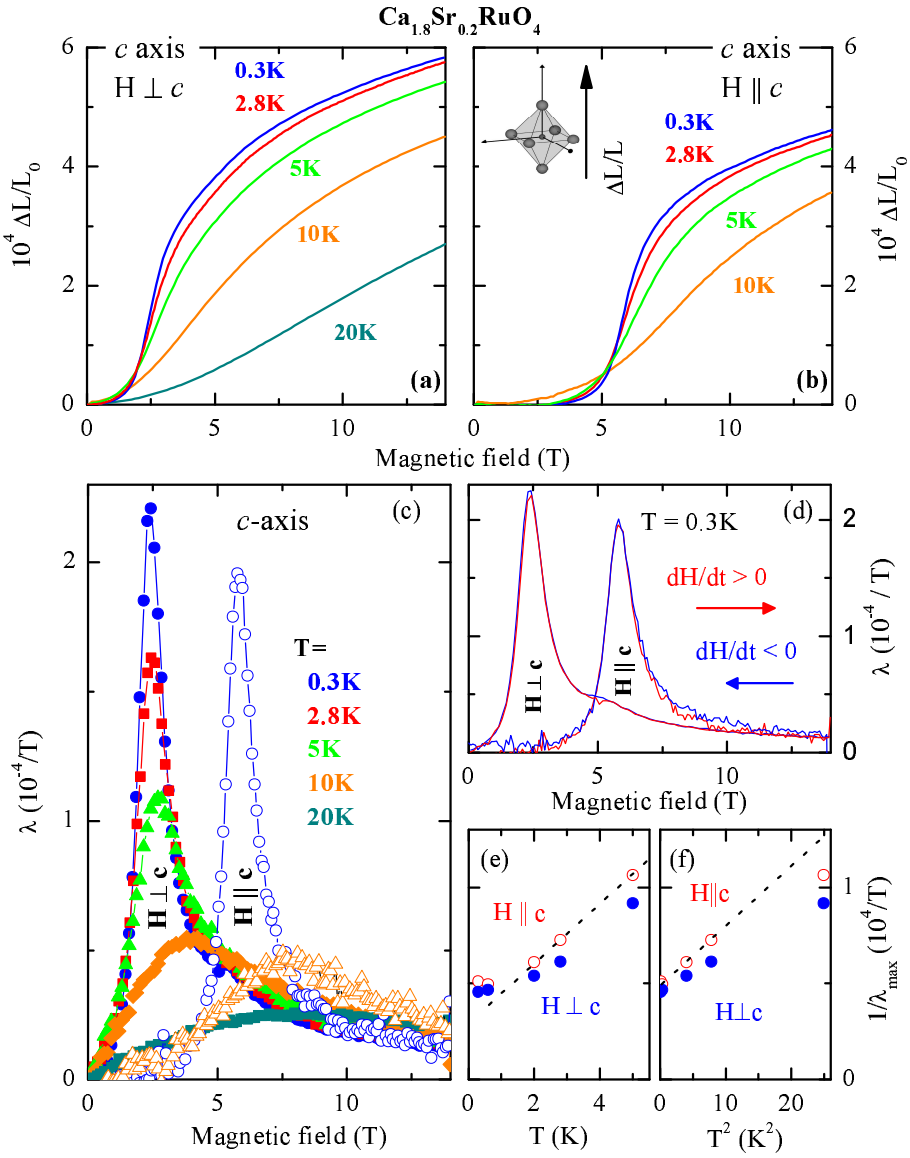

Fig. 3. Magnetostriction $\Delta L(H)/L_0$ along the c axis of $Ca_{1.8}Sr_{0.2}RuO_4$, measured in a field applied parallel (a) and perpendicular (b) to the c axis. Panel (c) displays the derivative $\lambda(H) = \frac{1}{L_0}\frac{\partial L}{\partial H}$ for the c axis in a magnetic field from selected measurements with $\mathrm{d}H/\mathrm{d}t > 0$. A comparison of $\lambda(H)$ for increasing ($\mathrm{d}H/\mathrm{d}t > 0$) and decreasing ($\mathrm{d}H/\mathrm{d}t < 0$) field is presented in panel (d). The inverse peak height $1/\lambda_{\max}$ of the $\lambda(H)$ anomaly at the metamagnetic transition is plotted versus T and T^2 in panel (e) and (f), respectively.

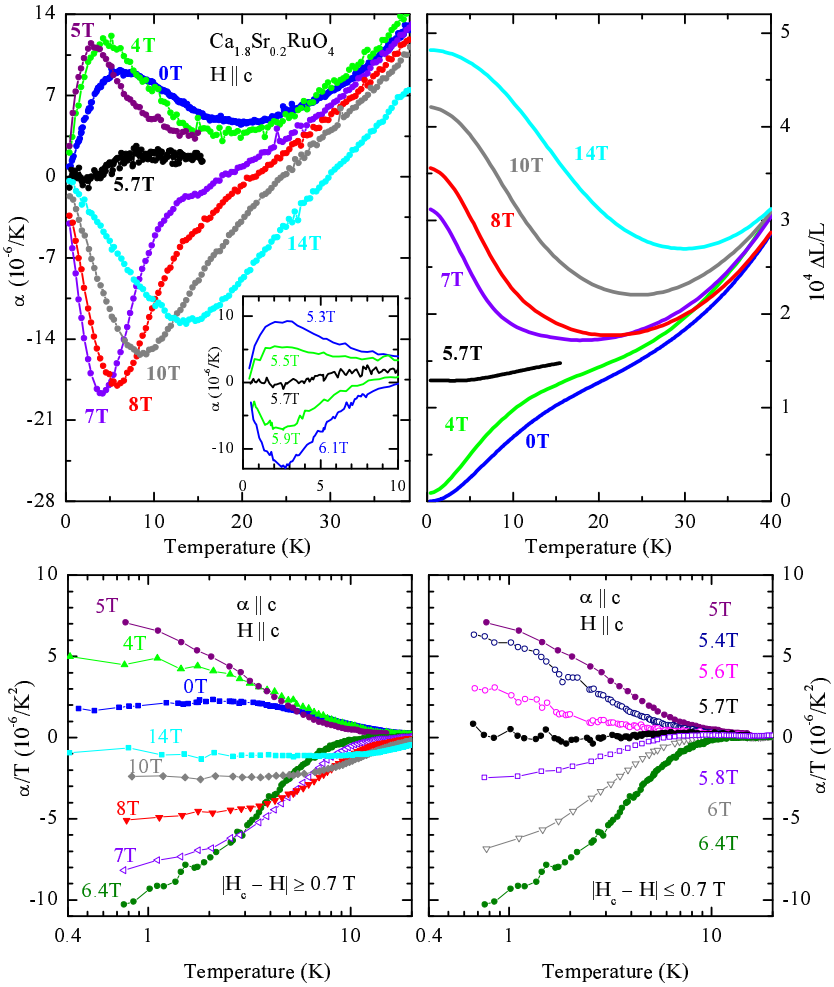

Fig. 4. Thermal expansion of $Ca_{1.8}Sr_{0.2}RuO_4$ parallel to the c axis in a longitudinal magnetic field. The upper left panel shows the thermal expansion coefficient $\alpha_c(T) = \frac{\partial c}{c \partial T}$ and the upper right panel the length change $\Delta c/c$ in fields below and above the metamagnetic transition at $H_c \simeq 5.7\,\mathrm{T}$. The inset shows a magnified view of the $\alpha_c(T)$ anomaly in the vicinity of the metamagnetic transition. In the lower panels, α_c/T is plotted on a logarithmic scale in fields far away from (left) and in the vicinity (right) of the metamagnetic transition.

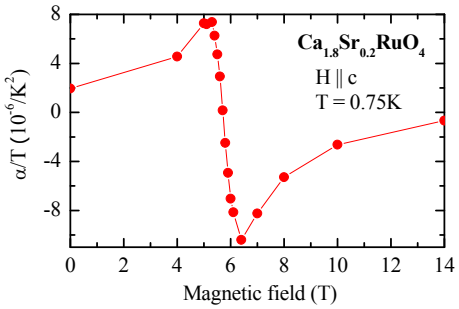

Fig. 5. The c-axis thermal-expansion coefficient divided by the temperature in $Ca_{1.8}Sr_{0.2}RuO_4$ as a function of the magnetic field.

can be related with the accumulation of entropy expected at the thermodynamic end-point. For $Sr_3Ru_2O_7$ it is argued that quantum criticality plays a dominant role in spite of the first-order character of the metamagnetic transition, since the end-point of the metamagnetic transition would be sufficiently low in temperature.[16,17,18] It is therefore interesting to look for signatures of a quantum-critical end-point in the thermodynamic properties of $Ca_{1.8}Sr_{0.2}RuO_4$ motivating us to extend the previous data[19] to lower temperatures. In the inset of the upper-left panel of Figure 4 we show the thermal expansion coefficient for magnetic fields close to the low-temperature metamagnetic transition. The anomalous effects seem to be essentially suppressed when approaching the transition field. This effect is also seen when plotting the ratio of the thermal expansion coefficient over temperature $\frac{\alpha_c(T)}{T}$, see the lower panels of Figure 4. Upon increase of the magnetic field $\frac{\alpha_c(T)}{T}$ first increases to exhibit maxima slightly below the metamagnetic transition, see Figure 5. At the transition it changes its sign and upon further field increase there is a minimum slightly above the transition. The absolute value of $\frac{\alpha_c(T)}{T}$ is roughly symmetric in $H - H_{mm}$ and the distance of the two extrema is in agreement with the width of the transition seen in the low-temperature magnetostriction. Dividing the $\frac{\alpha_c(T)}{T}$ values by the analogous $\frac{C_p(T)}{T}$ values one may determine the Grüneisen-parameter. The field dependence of the $\frac{C_p(T)}{T}$-ratio was reported in our previous paper.[19] Upon increasing the magnetic field at low temperature, $\frac{C_p(T)}{T}$ increases only by about 20% up to a maximum at the metamagnetic transition and then drops rapidly above the transition. Consequently, the Grüneisen-parameter does not diverge when approaching H_{mm} in $Ca_{1.8}Sr_{0.2}RuO_4$.

From inelastic neutron scattering, it is known that $Ca_{1.8}Sr_{0.2}RuO_4$ exhibits at least two magnetic instabilities[11,26] related with strongly enhanced magnetic fluctuations. An incommensurate antoferromagnetic contribution arising from Fermi-surface effects appears to compete with a quasi-

ferromagnetic instability. The latter can be directly deduced from the temperature dependence of the macroscopic susceptibility.[11,9] For compositions close to $Ca_{1.5}Sr_{0.5}RuO_4$ a ferromagnetic cluster glass has even been reported.[9] At intermediate temperatures the macroscopic susceptibility for $x = 0.2$ exceeds that of $Ca_{1.5}Sr_{0.5}RuO_4$ but it exhibits a maximum at around 10 K and is much smaller than that for $x = 0.5$ at low temperature. Compared to a Curie-Weiss extrapolation the susceptibility for $x = 0.2$ is significantly reduced at the lowest temperatures. The incipient ferromagnetic instability occurring in $Ca_{1.8}Sr_{0.2}RuO_4$ as well as in $Ca_{1.5}Sr_{0.5}RuO_4$ seems to get efficiently blocked through the structural anomaly flattening the RuO_6-octahedron at low temperatures. This effect may reduce the amplitude of the associated fluctuations and enhance their characteristic energy. Through the transfer of electrons into the γ-band, the ferromagnetic instability is weakened possibly due to a shift of the van-Hove singularity. At higher fields, the compound is forced into a ferromagnetic ordering and, therefore, quasi-ferromagnetic fluctuations are weakened by further stabilizing this ferromagnetic ordering explaining the reversed structural anomalies occurring upon cooling for fields above H_{mm}. The sign change of the thermal-expansion anomaly just at the transition field, its large amplitude and its nearly symmetric behavior around the transition field imply that the metamagnetic transition is related with strong fluctuations.[29] The critical end-point of the metamagnetic transition in $Ca_{1.8}Sr_{0.2}RuO_4$ although hidden by the intrinsic disorder of the system must be close within the relevant energy scales.

Garst and Rosch[29] and Gegenwart et al.[27] have made quantitative predictions for a metamagnetic transition related with a quantum-critical end-point which were already tested for the $Sr_3Ru_2O_7$-compound. First α/T should vary as $|H - H_{mm}|^{-\frac{4}{3}}$ at both sides of the transition. The $Ca_{1.8}Sr_{0.2}RuO_4$-data shown in Fig. 5 clearly deviate from such a behavior, in particular there is no divergence in the experimental data. Close to the transition the microscopic disorder may superpose positive and negative thermal expansion anomalies cancelling each other. The almost complete suppression of the anomaly close to the metamagnetic transition field is only possible if the intrinsic $\frac{\alpha}{T}(H - H_{mm})$ dependence is fully antisymmetric giving further weight to our interpretation that the strongest fluctuations appear just at the metamagnetic transition and that the critical end-point must be quite close. These theories furthermore correctly predict that the thermal expansion anomalies increase in temperature with increasing $|H - H_{mm}|$. However, the scaling laws proposed for the thermal expansion do not agree perfectly with our data.[30] Again the intrinsic disorder might change the temperature dependencies quite drastically. In addition the strong antiferromagnetic fluctuations which are well established in $Ca_{2-x}Sr_xRuO_4$ will also interfere with

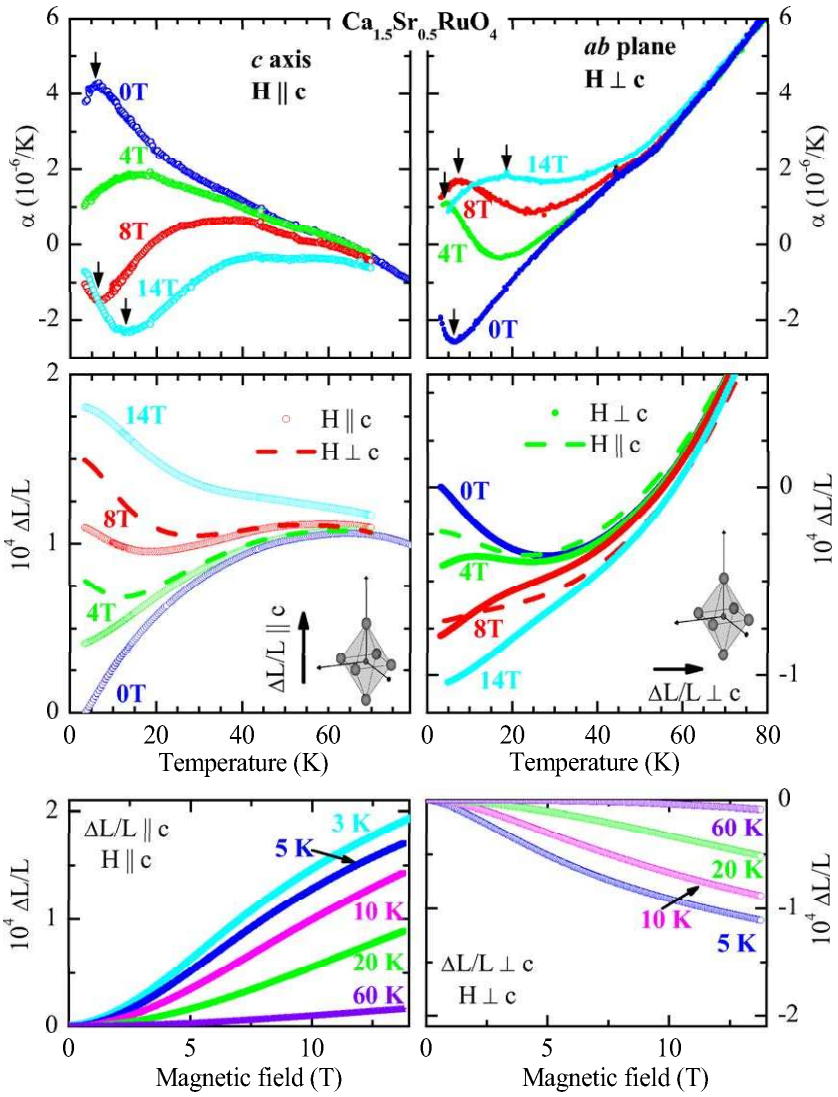

Fig. 6. Thermal expansion and magnetostriction of $Ca_{1.5}Sr_{0.5}RuO_4$ parallel (left) and perpendicular (right) to the c axis. The uppermost diagrams display $\alpha(T)$ for both directions, each with longitudinal applied magnetic field. The corresponding length change $\Delta L/L$ is presented below. These diagrams show additionally the results obtained from measurements in transverse magnetic field as broken lines. The lowermost panels show the magnetostriction, each recorded in longitudinal applied magnetic field.

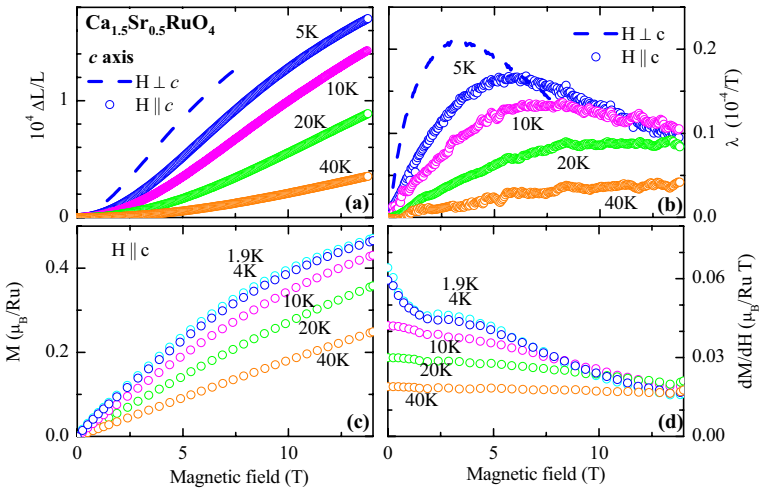

Fig. 7. Comparison of the anomalous behavior of the c-axis magnetostriction (upper panels) and the magnetization (lower panels) for $Ca_{1.5}Sr_{0.5}RuO_4$. On the right, the data obtained from measurements in a magnetic field applied along c direction are shown. The diagrams on the left display the corresponding derivative. The broken line in the upper panels represent an example of the magnetostriction in a magnetic field perpendicular to the c axis.

the thermodynamic parameters.

3.2. Magnetism in $Ca_{1.5}Sr_{0.5}RuO_4$

Concerning the crystal structure, $Ca_{1.5}Sr_{0.5}RuO_4$ differs from the $Ca_{1.8}Sr_{0.2}RuO_4$-compound by the absence of the long-range tilt distortion. This is visible in the c-axis thermal-expansion coefficient which is negative over a wide temperature interval, see Figure 1. Due to the larger and positive thermal-expansion coefficient in the a, b plane the volume thermal expansion however is positive also for $x = 0.5$. Taking into account the different thermal expansion behavior at intermediate temperatures, the low-temperature c-axis anomalies are qualitatively similar in $Ca_{1.8}Sr_{0.2}RuO_4$ and in $Ca_{1.5}Sr_{0.5}RuO_4$, compare Figures 6 and 4. This suggests that a metamagnetic transition also occurs in $Ca_{1.5}Sr_{0.5}RuO_4$. However, all structural anomalies are significantly smaller for $x = 0.5$. The field-dependent thermal expansion for $x = 0.5$ was measured in the four configurations with field and length change either parallel or perpendicular to the c-axis. Again the difference in the longitudinal and transverse configurations arise mainly from a shift in the transition fields which is much smaller for fields oriented perpendicular to the c-axis. In addition to the results discussed for $x = 0.2$, these

$Ca_{1.5}Sr_{0.5}RuO_4$-data show that the in-plane lattice parameters anomalously increase upon cooling in zero field and become shorter in high fields. The magnetostriction data shown in the lowest panels of Figure 6 confirm the opposite signs of the field-induced length changes parallel and perpendicular to the c-axis. The volume magnetostriction is about an order of magnitude smaller than the uniaxial components confirming our interpretation that these effects arise from an orbital rearrangement between the t_{2g}-orbitals.[19] The strong reduction of the magnetostriction and of the thermal expansion anomalies for $x = 0.5$ must be related with the absence of the long-range tilt deformation. Either the lattice in the crystal structure with a simple rotational distortion is much harder thereby reducing the structural response, or there is a direct interplay between the tilt and electronic parameters. One may expect the tilt deformation to act more strongly on the d_{xz} and d_{yz} orbitals in contrast to the octahedron rotation which interferes mostly with the d_{xy} orbitals.[5,6]

Figure 7 compares the magnetization and the field-induced length change along the c-direction and their derivatives versus magnetic field. In the magnetization hysteresis cycles we find a remanent magnetization of a few thousands of a μ_B for fields along and perpendicular to the c-direction in agreement with the cluster-glass behavior reported in reference.[9] The underlying short-range ferromagnetic ordering seems to be another consequence of the intrinsic disorder implied by the Ca/Sr mixing. Even though the remanent magnetization is extremely small the underlying ferromagnetic ordering has a strong impact on the magnetization curves, in particular for the field within the planes. At low field the magnetization sharply increases hiding any metamagnetic transition at higher field. The magnetization data shown in Figure 7 do not yield direct evidence for the metamagnetic transition. Furthermore, the steep low-field increase of the magnetization is not accompanied by the magnetostriction in contrast to the close coupling between these entities in $Ca_{1.8}Sr_{0.2}RuO_4$. The low-field increase of the magnetization seems to fully arise from the short-range ferromagnetic correlations; this feature is not related with the metamagnetic transition and there is no comparable feature observed for $x = 0.2$. However, the field derivative of the magnetization for $Ca_{1.5}Sr_{0.5}RuO_4$ shown in the lower-right panel of Figure 7 clearly exhibits two features: in addition to the finite low-field value there is a clear shoulder at higher fields resembling the peak at the metamagnetic transition in $Ca_{1.8}Sr_{0.2}RuO_4$. This second feature corresponds to the maximum in the magnetostriction (upper right panel). Therefore, we may conclude that a metamagnetic transition in $Ca_{1.5}Sr_{0.5}RuO_4$ still occurs, although the associated jump in the magnetization is strongly reduced compared to that in the $Ca_{1.8}Sr_{0.2}RuO_4$.

4. Conclusions

Detailed studies of the structural properties in $Ca_{1.8}Sr_{0.2}RuO_4$ and in $Ca_{1.5}Sr_{0.5}RuO_4$ by diffraction and by dilatometer methods allow us to clarify the microscopic and the thermodynamic aspects of the metamagnetic transition in these materials. A temperature and magnetic-field driven redistribution of the orbital occupation seems to be responsible for the anomalous structural effects. Upon cooling in zero field $3d$-electrons seem to move into the d_{xy} orbitals causing a suppression of a quasi-ferromagnetic instability. This effect is reversed either by cooling at high magnetic field or by applying a magnetic field at low temperature. The structural difference between $Ca_{1.8}Sr_{0.2}RuO_4$ and $Ca_{1.5}Sr_{0.5}RuO_4$ consists in the long-range tilt deformation which is found to strongly enhance the structural as well as the magnetic anomalies. Even though the magnetization data in $Ca_{1.5}Sr_{0.5}RuO_4$ do not exhibit the well-defined metamagnetic transition, the field derivative of the magnetization as well as the magnetostriction clearly show that a qualitatively similar metamagnetic transition also occurs in $Ca_{1.5}Sr_{0.5}RuO_4$. However, this material already exhibits short-range ferromagnetic ordering at low temperature and zero magnetic field which partially hides the metamagnetic transition. The identical ferromagnetic instability is also present in $Ca_{1.8}Sr_{0.2}RuO_4$ at intermediate temperature, but here it is fully suppressed at low temperature due to the octahedron tilting.

By analyzing the thermal expansion anomalies close to the metamagnetic transition in $Ca_{1.8}Sr_{0.2}RuO_4$, we present evidence that the related critical end-point must be close to the low-temperature transition in the relevant scales. In particular, we find that the α/T-coefficient is nearly symmetric across the transition field. The more precise scaling predictions for the thermal expansion coefficient across a metamagnetic transition are, however, not fulfilled in $Ca_{1.8}Sr_{0.2}RuO_4$. In this material intrinsic disorder as well as the competition of different magnetic instabilities appear to play an important role.

ACKNOWLEDGMENTS

We wish to dedicate this manuscript to Professor Hilbert von Löhneysen on the occasion of his 60th birthday. He has made numerous contributions to the field of strongly correlated electron systems and quantum phase transitions from which we all have greatly benefited. This work was supported by the DFG through the Sonderforschungsbereich 608.

REFERENCES

1. Y. Maeno, H. Hashimoto, K. Yoshida, S. Nishizaki, T. Fujita, J.G. Bednorz, and F. Lichtenberg, Nature **372**, 532 (1994).
2. A.P. Mackenzie and Y. Maeno, Review of Modern Phys. **75**, 657 (2003).
3. S. Nakatsuji et al., J. Phys. Soc. Jpn. 66, 1868 (1997); S. Nakatsuji and Y. Maeno, *Phys. Rev. Lett.* **84**, 2666 (2000).
4. M. Braden et al., Phys. Rev. B **58**, 847 (1998a).
5. Z. Fang K. Terakura, Phys. Rev. B **64**, 020509 (2001).
6. Z. Fang and N. Nagaosa and K. Terakura, Phys. Rev. B **69**, 045116 (2004).
7. O. Friedt, M. Braden, G. André, P. Adelmann, S. Nakatsuji, and Y. Maeno, Phys. Rev. B **63**, 174432 (2001).
8. S. Nakatsuji and Y. Maeno, *Phys. Rev. B* **62**, 6458 (2000).
9. S. Nakatsuji, D. Hall, L. Balicas, Z. Fisk, K. Sugahara, M. Yoshioka, and Y. Maeno, *Phys. Rev. Lett.* **90**, 137202 (2003).
10. R. Jin et al., cond-mat0112405.
11. O. Friedt, P. Steffens, M. Braden, Y. Sidis, S. Nakatsuji, and Y. Maeno,*Phys. Rev. Lett.* **93**, 147404 (2004).
12. Y. Sidis, M. Braden, P. Bourges, B. Hennion, S. NishiZaki, Y. Maeno, and Y. Mori, Phys. Rev. Lett. **83**, 3320 (1999).
13. M. Braden, Y. Sidis, P. Bourges, P. Pfeuty, J. Kulda, Z. Mao, and Y. Maeno, Phys. Rev. B **66**, 064522 (2002).
14. V.I. Anisimov et al., Eur. Phys. J. B25, 191 (2002).
15. L. Balicas, S. Nakatsuji, D. Hall, T. Ohnishi, Z. Fisk, Y. Maeno, and D.J. Singh, Phys. Rev. Lett. **95**, 106407 (2005).
16. R.S. Perry et al., Phys. Rev. Lett. 86, 2661 (2001).
17. S.A. Grigera et al., Science 294, 329 (2001).
18. S.A. Grigera, P. Gegenwart, R.A. Borzi, F. Weickert, A.J. Schofield, R.S. Perry, T. Tayama, T. Sakakibara, Y. Maeno, A.G. Green, and A.P. Mackenzie, Science **306**, 1154 (2004).
19. M. Kriener, P. Steffens, J. Baier, O. Schumann, T. Zabel, T. Lorenz, O. Friedt, R. Müller, A. Gukasov, P. Radaelli, P. Reutler, A. Revcolevschi, S. Nakatsuji, Y. Maeno and M. Braden, Phys., Rev. Lett. **95**, 267403 (2005).
20. J. Baier, T. Tabel, M. Kriener, P. Steffens, O. Schumann, O. Friedt, A. Freimuth, A. Revcolevschi, S. Nakatsuji, Y. Maeno, T. Lorenz and M. Braden, Physica B **378**, 497 (2006).
21. S. Nakatsuji and Y. Maeno, *J. Solid State Chem.* **156**, 26 (2001).
22. G. Brändli and R. Griessen, Cryogenics **13**, 299 (1973).
23. T. Lorenz, U. Ammerahl, B. Büchner, and A. Revcolevschi, Phys. Rev. B **55**, 5914 (1997).
24. R. Pott and R. Schefzyk, J. Phys. E – Sci. Instrum. **16**, 444 (1983).
25. O. Heyer, Diploma Thesis, University of Cologne (2006).
26. P. Steffens et al., unpublished results.
27. P. Gegenwart, F. Weickert, M. Garst, R.S. Perry, and Y. Maeno, Phys. Rev. Lett. **96**, 136402 (2006).
28. J. Zhang, Ismail, R.G. Moore, S.-C. Wang, H. Ding, R. Jin, D. Mandrus, and E.W. Plummer Phys. Rev. Lett. **96**, 066401 (2006).

29. M. Garst and A. Rosch, Phys. Rev. B **72**, 205129 (2005).
30. J. Baier, PhD-thesis, University of Cologne (2006).